Imitation Learning-based Control of Brachiation Motion with Anthropomorphic Hands

Anubhav Tripathi[1*] and Nagamanikandan Govindan[2] and Harikumar Kandath[1]

[1]Robotics Research Center, IIIT Hyderabad, India
Hyderabad, 500032, India (anubhav.tripathi@research.iiit.ac.in)* Corresponding author
[2]Department of Mechanical Engineering, IIITDM Kancheepuram,
Kancheepuram, 600127, India (nagamanikandan.g@iiitdm.ac.in)

Abstract: Brachiation, inspired by ape locomotion, involves swinging from one substrate to another. Existing approaches typically rely on simple grippers and computationally expensive optimal control to compute feasible states and control trajectories. In contrast, learning-based methods often lack physical modeling and require extensive training data. We present a brachiating system using high degree-of-freedom anthropomorphic hands to generate swing trajectories and perform stable grasps in a physics-based simulation environment (MuJoCo). An optimal open-loop trajectory is first generated via trajectory optimization based on a desired grasp location. A tracking controller follows this reference, while a grasping controller activates upon proximity to ensure secure contact. To reduce computational cost, we train a Generative Adversarial Imitation Learning (GAIL) policy using expert trajectories from the optimization framework. The GAIL-based controller generalizes to perturbed conditions and eliminates the need for repeated re-optimization, significantly lowering computation time. It also adapts to varying initial configurations, removing the requirement to rerun optimization for each case. We compare the learned model with a traditional optimal controller and demonstrate marked improvements in both computational efficiency and versatility.

Keywords: Brachiation, Anthropomorphic Hand, Trajectory Optimization, GAIL, PD, MuJoCo

1. INTRODUCTION

Brachiation, inspired by the arm-swinging locomotion of primates, offers a promising approach for robotic traversal in unstructured or elevated environments. Unlike bipedal or wheeled locomotion, brachiating robots swing between fixed supports, enabling motion in forests, power lines, or space habitats where traditional mobility fails.

Over the years, brachiation control has evolved from energy-based swing-up strategies like partial feedback linearization [1], to hybrid controllers integrating target dynamics and energy shaping [2], and more recently, learning-based methods such as Tarzan [3], AcroMonk [4], and imitation-driven models [5]. However, these systems typically rely on underactuated arms and low-DOF grippers, often treating grasping and swing control as separate modules.

In contrast, we propose a high-DOF brachiation robot composed of a two-link robot and two 16-DOF Anthropomorphic Hands. Our framework combines offline trajectory optimization for swing planning with a real-time data-driven grasp controller, triggered by spatial proximity. Once a secure grasp is made, the prior hand releases—enabling continuous brachiation.

We evaluate two swing control strategies: a precise PD controller tracking optimized joint trajectories, and a GAIL[6]-based policy trained on expert demonstrations with parameter perturbations. For grasping, a regression model trained on successful grasp data enables robust 16-DOF torque control, allowing interaction with cylindrical substrates of varying sizes.

The proposed system is validated in MuJoCo simulations across single and dual-swing scenarios.

Key contributions:

- Design and simulation of a 35-DOF brachiating robot with high-DOF anthropomorphic grippers.
- Hybrid control framework integrating swing trajectory optimization, imitation learning, and learned grasp control.
- Coordinated dual-arm sequencing for seamless grasp release transitions.
- Performance evaluation comparing PD and GAIL-based swing controllers in simulation.

This work lays the groundwork for scalable, adaptive brachiating robots capable of operating in both structured and dynamic environments. Future extensions include learning-based control, variable spacing, and full 3D brachiation.

2. RELATED WORK

Early brachiation control used heuristic and neural-inspired methods. One early study applied CMAC to generate control inputs without precise dynamic models [7], establishing the foundation for model-free approaches.

The Acrobot swing-up problem became a canonical underactuated control benchmark. Spong's controllers used partial feedback linearization and Lyapunov techniques to regulate system energy [8], [1], influencing later methods in dynamic locomotion.

Nakanishi et al. proposed hybrid controllers combining target dynamics with energy shaping to improve robustness against initial condition variability [2]. Their target dynamics method encoded brachiation as a harmonic oscillator-based limit cycle, enabling hardware demonstrations on swing, ladder, and rope locomotion [9],[10].

Gomes and Ruina [11] modeled a five-link 2D ape to

explore zero-energy-cost brachiation using passive dynamics, offering biomechanical insights and energy-efficient motion strategies.

Fukuda et al. introduced PDAC with Virtual Holonomic Constraints for Gorilla Robot III, reducing energy consumption by leveraging joint symmetry and passive dynamics [12]. Nakanishi and Vijayakumar [13] used Variable Stiffness Actuation (VSA) to jointly optimize stiffness and timing, improving dynamic swing robustness.

Tarzan [3] showcased wire-borne brachiation using wrist rotation and locking grippers for efficient 2D movement, suggesting potential for agricultural and inspection tasks. Farzan et al. [14] used adaptive robust control to compensate unknown cable dynamics in flexible settings.

Yang et al. [15] presented a three-link robot with iLQR-based trajectory generation and cascaded PID + input-output linearization tracking, improving swing stability with lightweight design. AcroMonk [4], a minimalist underactuated robot, demonstrated swing stabilization using trajectory optimization, TVLQR, and RL under uncertainties. A recent work by Fukaya et al. [16] introduced a single-rod brachiation robot with a simplified structure, achieving aerial brachiation over multiple bars. Reda et al. [5] proposed an imitation-driven framework where a policy trained on a simplified model controls a 14-link robot, enabling dynamic swings and emergent back-and-forth behaviors.

While some systems like Tarzan [3] and those based on target dynamics [10] employed active grippers, they typically relied on low-DOF designs and treated grasping as a separate task. In contrast, our work introduces a unified control framework that synchronizes swing and grasp actions using high-DOF anthropomorphic hands. This combination of offline swing trajectory optimization and a proximity-triggered, data-driven grasp controller enables coordinated multi-swing brachiation in simulation, addressing a gap in existing literature.

3. METHODOLOGY

In this work, we develop and simulate a brachiation robot that combines an underactuated acrobot structure with dual Anthropomorphic Hands acting as grippers at both ends. The goal is to achieve rhythmic brachiation-like locomotion by swinging from one fixed substrate to the next, using coordinated dynamics and grasping control. Figure 1 shows the initial and final configurations during one complete brachiation cycle, from the start of swing to substrate grasp.

Fig. 1. Initial and final configurations at the start and end of a single brachiation cycle.

3.1 System Description and Mathematical Model

Our robot consists of a two-link underactuated acrobot with anthropomorphic Allegro Hands (16 DOF each) mounted at both ends. Each link and attached hand has a combined mass of approximately $1.1\ kg$. The anthropomorphic Hands are used for dynamic grasping of cylindrical substrates placed in the environment. For trajectory generation, we use a simplified model that ignores the high-DOF hands and considers only the two-link acrobot, which is sufficient for generating effective swing trajectories.

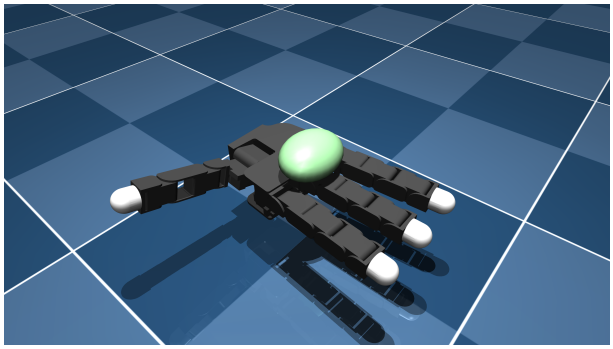

Fig. 2. An anthropomorphic hand (Allegro Hand) used for grasping the substrate.(Source:Mujoco Menagerie [17])

The simplified planar acrobot dynamics are governed by the Euler–Lagrange equation:

$$\mathbf{M}(\mathbf{q})\,\ddot{\mathbf{q}} + \mathbf{C}(\mathbf{q},\dot{\mathbf{q}})\,\dot{\mathbf{q}} + \mathbf{G}(\mathbf{q}) = \mathbf{B}\,\mathbf{u}, \tag{1}$$

where $q = [q_1, q_2]^T$ are the shoulder and elbow joint angles, and u is the actuation torque applied at the elbow joint. We define the full system state as:

$$x = \begin{bmatrix} q \\ \dot{q} \end{bmatrix} = [q_1, q_2, \dot{q}_1, \dot{q}_2]^T. \tag{2}$$

Here, $\mathbf{M}(\mathbf{q}) \in \mathbf{R^{2\times 2}}$ is the inertia matrix, $\mathbf{C}(\mathbf{q},\dot{\mathbf{q}}) \in \mathbf{R^{2\times 1}}$ is the Coriolis/centrifugal vector, and $\mathbf{G}(\mathbf{q}) \in \mathbf{R^{2\times 1}}$ is the gravity vector. $\mathbf{B} \in \mathbf{R^{2\times 1}}$ is the actuation matrix, and $u \in R$ is the control input torque.

Simplified Model for Trajectory Generation: The trajectory optimization problem described in Sec. 3.1 is based on this simplified two-link model and excludes the dynamics of the Allegro Hands. Once an optimal state-control sequence $\{x^*(t), u^*(t)\}$ is obtained, it is applied to the full MuJoCo model, which includes both 16-DOF Allegro Hands. Despite ignoring the added inertia from the hands during optimization, the simplified model remains effective in practice. The high-DOF hands slightly perturb the system's swing behavior, but our PD tracking controller (Sec. 3.2) compensates for these deviations, enabling robust swing-and-grasp execution in simulation.

Trajectory Optimization via Trapezoidal Collocation: We discretize the infinite-dimensional optimal control problem into an N-point nonlinear program by defin-

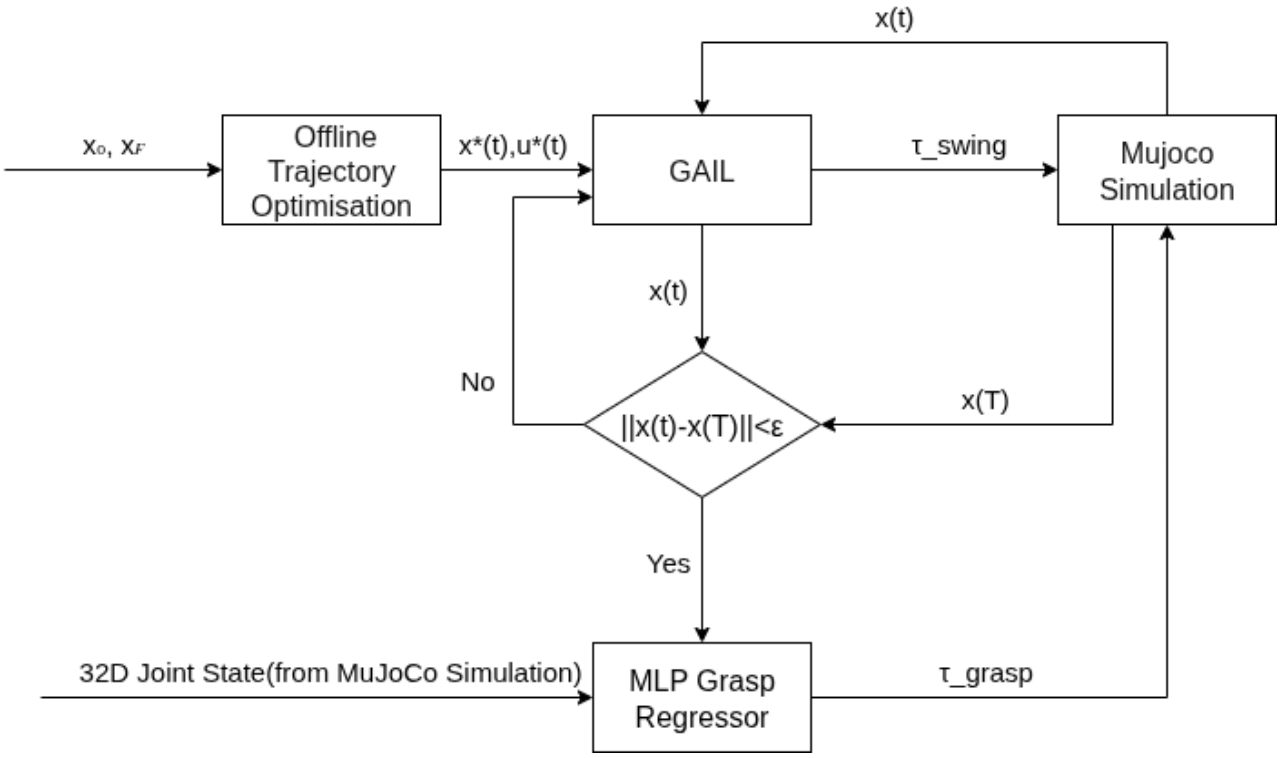

Fig. 3. Block diagram of GAIL-based brachiation control. The policy is trained using optimized trajectories. A proximity-triggered MLP regressor generates grasp torques. Simulation provides feedback for GAIL.

ing:

$$t_k = \frac{k-1}{N-1}\,T, \quad x_k \approx x(t_k), \quad u_k \approx u(t_k),$$
$$f_k = f(x_k, u_k), \quad \Delta t = \frac{T}{N-1},$$

where $f(x_k, u_k)$ represents the system dynamics at the k-th discretization point.

The continuous cost function,

$$J = \int_0^T \|u(t)\|^2 \,\mathrm{dt}, \tag{3}$$

is approximated using the trapezoidal rule:

$$J \approx \sum_{k=1}^{N} w_k \,\|u_k\|^2 \,\Delta t, \quad w_k = \begin{cases} \frac{1}{2}, & k = 1 \text{ or } k = N, \\ 1, & \text{otherwise.} \end{cases} \tag{4}$$

System dynamics are enforced via defect constraints using trapezoidal integration:

$$x_{k+1} - x_k - \tfrac{\Delta t}{2}\left(f_k + f_{k+1}\right) = 0, \quad k = 1, \ldots, N-1. \tag{5}$$

Including terminal constraints and bounded control inputs, the final nonlinear program becomes:

$$\begin{aligned} \min_{x_{1:N},\, u_{1:N}} \quad & \sum_{k=1}^{N} w_k \,\|u_k\|^2 \,\Delta t \\ \text{s.t.} \quad & x_{k+1} - x_k - \tfrac{\Delta t}{2}\left(f(x_k, u_k) + f(x_{k+1}, u_{k+1})\right) = 0, \\ & x_1 = x_0, \quad x_N = x_F \quad \text{(initial and terminal constraints)}, \\ & u_{\min} \le u_k \le u_{\max}, \quad k = 1, \ldots, N. \end{aligned} \tag{6}$$

3.2 Control Architecture

Our three-stage controller (Fig. 3) combines the strengths of offline optimization, high-level tracking controller, and low-level grasp/release logic:

1. **Offline Trajectory Optimization:** Using trapezoidal direct collocation via optimTraj and MATLAB's `fmincon`, we solve an energy-minimizing Brachiation motion problem (Eq. (3)), producing reference trajectories $x^*(t), u^*(t)$. Since the optimization is performed on a simplified two-link acrobot model without the anthropomorphic hands, the resulting $u^*(t)$ cannot be directly applied to the full system.

2. **High-Level Tracking Controller:** We implement two swing controllers: a PD controller and a GAIL-based policy. The PD controller directly tracks a single offline-optimized trajectory obtained from trajectory optimization. For the PD controller, the joint torque command is computed as

$$\tau = K_p\left(q_{\text{des}} - q\right) + K_d\left(\dot{q}_{\text{des}} - \dot{q}\right), \tag{7}$$

where q and $\dot{q}$ are the measured joint angles and angular velocities, and q_{des}, $\dot{q}_{\text{des}}$ are obtained from the offline-optimized trajectory at each time step. The PD gains were tuned empirically to balance stability and responsiveness. Torque commands are constrained within experimentally chosen safety limits to prevent unrealistic actuator behavior in simulation. The controller operates synchronously with the MuJoCo simulation step, ensuring real-time tracking of the desired trajectory.

Alongside the PD controller, we introduce a Generative Adversarial Imitation Learning (GAIL)–based policy that

learns to replicate expert behavior through adversarial training. The GAIL policy is modeled as a two-layer multilayer perceptron (MLP) with 128 hidden units per layer and ReLU activations, outputting Gaussian-distributed torques based on a 5D input state $[t, \theta_1, \theta_2, \dot{\theta}_1, \dot{\theta}_2]$. A discriminator network distinguishes expert actions from agent-generated behavior. GAIL is trained on 70 expert trajectories (generated under varied initial conditions and dynamics) for 400 epochs using REINFORCE-style updates with discriminator-derived rewards. Fig. 4 illustrates the architecture used during GAIL training, where the generator interacts with the MuJoCo simulator and the discriminator distinguishes expert and generated trajectories. The GAIL training process includes feedback from MuJoCo simulation (state trajectories), forming an adversarial loop between policy and discriminator.

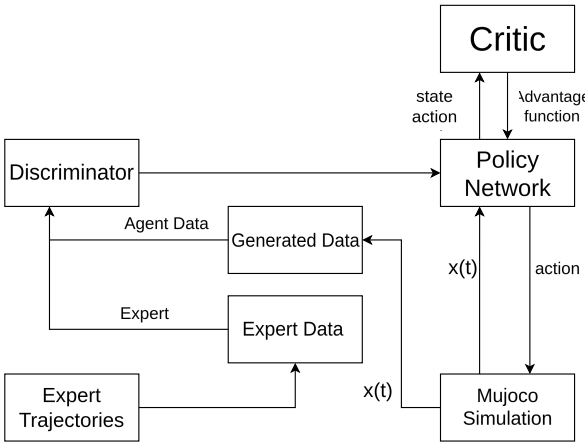

Fig. 4. GAIL architecture: The discriminator is trained to distinguish expert and generated data, while the generator (policy) interacts with the MuJoCo simulation. Generated and expert data flow into the discriminator to drive adversarial learning.

During execution, the GAIL policy outputs joint torque commands directly at each simulation step, which are then bounded within safe torque limits before being applied to the actuators. Once trained, the GAIL policy generates control actions in real time without requiring trajectory re-optimization. It exhibits better generalization to perturbed initial states than PD control but consumes more energy and has a lower grasp success rate. This trade-off makes GAIL more suitable for dynamic and uncertain environments requiring real-time adaptability.

3. **Low-Level Grasp/Release:** The low-level grasp controller is activated based on proximity to the swing target. Let $x(T)$ be the desired end-effector position at grasp time. During the swing, the Euclidean distance $\|x_{\text{current}} - x(T)\|$ is monitored, and when this falls below a threshold $\epsilon = 0.10\,\text{m}$, the grasp sequence is initiated. Upon activation, a trained regression model maps the 32-dimensional joint state of the Anthropomorphic Hand (16 joint positions + 16 joint velocities) to 16 output torques, enabling full-DOF grasping. The model is implemented as a multilayer perceptron (MLP) regressor with two hidden layers of 64 neurons each and ReLU activations. It is trained using the Adam optimizer on successful grasp trajectories collected in simulation. If the proximity threshold is not met ("No" case in Fig. 3), the system continues executing the swing controller until the condition is satisfied. This integrated control architecture enables coordinated swing and grasp actions, forming the basis for the performance evaluation presented in the following section.

Sequential Execution: This sequence is repeated for each swing, forming a closed loop of coordinated swinging and grasping actions that result in robust multi-phase brachiation behavior.

4. SIMULATION EXPERIMENTS AND RESULTS

All simulations are conducted in the MuJoCo physics engine, which provides accurate modeling of joint dynamics, contact forces, and actuation. The robot model includes explicit link masses, joint constraints, and hand-substrate interaction.

To evaluate our brachiation controller, we conducted a series of MuJoCo simulation trials using the optimized swing trajectory and real-time coordinated swing–grasp controller described in Section 3.2. These experiments validate robustness across single and dual-swing scenarios.

To improve robustness, the expert dataset includes ±20% link mass variation, ±10° joint angle perturbation, and ±3 cm link length offsets. The trained GAIL controller performs reliably within this distribution. However, the overall grasp success rate—measured across both in-distribution and out-of-distribution perturbations—is approximately 58%, with performance degrading as deviations increase.

4.1 Training Dynamics and Analysis

Figure 5 shows the training curve of the GAIL controller. Over 400 epochs, the discriminator loss steadily decreases while the generator (policy) stabilizes, indicating successful convergence. This behavior reflects that the policy increasingly generates trajectories similar to expert demonstrations, eventually reaching a near-equilibrium between discriminator and generator. The adversarial feedback loop, along with exposure to diverse initial conditions, supports robust policy learning under model uncertainty.

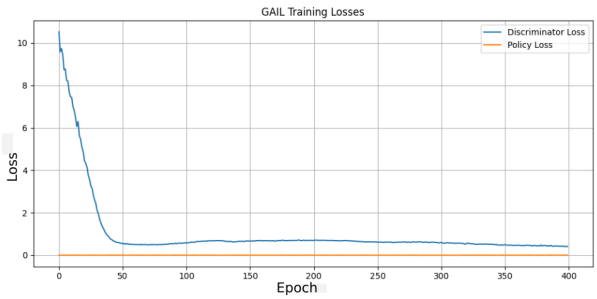

Fig. 5. Training process of the GAIL-based controller using expert trajectories and simulated feedback.

4.2 Single-Swing Timing

In each trial, the robot begins in the initial posture $(q_1, q_2) = (-45°, -90°)$, swings to the next substrate posture $(+45°, +90°)$, and executes the grasp/release cycle. We observed:

- **Swing duration:** The shoulder and elbow joints complete the prescribed trajectory in ≈ 2.0 s for GAIL and less than that for PD. The PD controller required 29.77s to compute each optimal trajectory on an NVIDIA GeForce RTX 3060 GPU, limiting its use in real-time scenarios where rapid re-planning is needed (1–2s per swing). To address this limitation, we adopt Generative Adversarial Imitation Learning (GAIL) which is online and robust to perturbations.
- **Grasp hold:** Upon contacting the next bar, the Anthropomorphic Hand closes and holds for a second to secure grasp.
- **Release delay:** After the hold, the opposite hand releases immediately, enabling the next swing.

4.3 Multi-Swing Performance

We ran two consecutive swings in a single continuous trial to test transition robustness. Over these 2 swings:

- **Success rate:** All the swings successfully reached and grasped the next substrate without slipping in PD-based swing control while success rate reduces when GAIL is used for swing.
- **Trajectory tracking:** The robot successfully follows the optimized swing trajectory across multiple phases, as observed through consistent motion profiles and substrate grasp success. This indicates reliable execution of the planned path within the dynamic limits of the system.
- **Cycle time:** Each full brachiation cycle (swing + hold + release) completed within 3.0 s.

4.4 Discussion and Conclusion

The controller completed each swing in 2s, followed by a 1s grasp phase. PD showed high success by accurately tracking trajectories despite added gripper mass and underactuation. Its 100% success rate across multiple swings reflects reliable coordination between swing and grasp subsystems.

In contrast, the GAIL-based swing controller improves robustness and generalization. Notably, it enables the system to **recover from perturbed initial joint configurations**, where PD often fails. This enhanced adaptability comes at a cost—GAIL consumes more energy and achieves a lower grasp success rate due to suboptimal early-phase motions and longer cycle durations. The GAIL policy does not explicitly track a reference trajectory, unlike PD, but learns swing dynamics directly from data, contributing to its flexibility. Future work will focus on optimizing this trade-off between robustness and efficiency.

Moreover, the combination of trajectory optimization with learning-based control provides a promising hybrid framework. The use of anthropomorphic hands also opens avenues for studying fine-grained manipulation during dynamic motion. We also plan to extend our framework to 3D brachiation with lateral maneuvers and adaptive bar spacing.

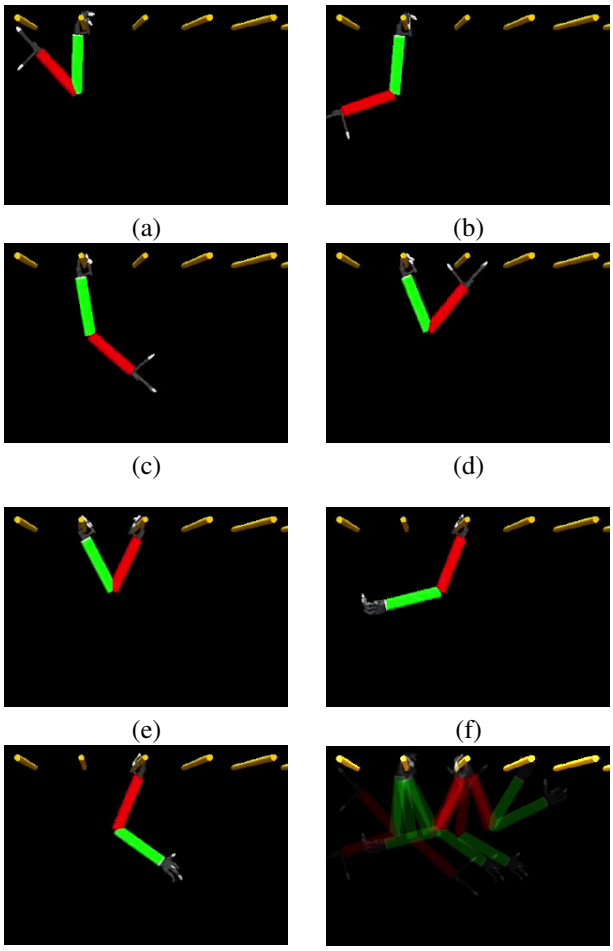

Fig. 6. Sequential snapshots of brachiation motion at various instants with final motion trail across two swings.

Table 1. Performance comparison between PD and GAIL swing controllers. GAIL demonstrates superior recovery from perturbed initial states at the cost of energy efficiency and success rate.

Metric (per swing)	**PD**	**GAIL**
Control Mode	Offline	Online
Recovery from Perturbed Initial State	Poor	Better
Computation Time (per Trajectory)	30 s	0.00008 s
Grasp Success Rate	100%	58%
Energy Usage	19.5 J	100 J
Time per Swing Cycle	1.286 s	2 s

5. FUTURE WORK

The current approach uses offline-optimized trajectories and PD-based tracking, which ensures high accuracy but may not generalize well to perturbations. In contrast, our preliminary results with a GAIL-based online controller show improved adaptability but lower grasp accuracy and significantly higher energy consumption. As a next step, we aim to improve the **accuracy and energy**

efficiency of the online imitation-based controller, enabling robust and sustainable brachiation under dynamic and uncertain conditions. This includes optimizing policy structure, tuning reward shaping for energy minimization, and incorporating curriculum learning for complex initializations. Reducing energy consumption while maintaining robust trajectory tracking under perturbations will be the key focus of future improvements.

Second, our current system assumes that the spacing between substrates lies within the robot's reachable range. To overcome this limitation, we plan **ricochetal brachiation**, involving large-amplitude swings that leverage momentum to reach substrates beyond static reach. Future work will also explore three or more consecutive swings to strengthen grasp reliability in extended motion sequences, especially under perturbation. Incorporating online feedback for grasp quality estimation and recovery will be investigated to address second-swing failures.

Currently, the system supports planar (2D) brachiation only. Future work includes **3D brachiation** with lateral transitions to navigate cluttered structures like trees, pipelines, or industrial scaffolding. Additionally, simulation-to-real transfer strategies will be explored using domain randomization, torque-limited policies, and fine-tuning with hardware-in-the-loop experiments.

Together, these enhancements aim to take a significant step toward deploying high-DOF brachiation robots in real-world, unstructured environments where robust, adaptive, and energy-aware locomotion is critical.

REFERENCES

[1] M. W. Spong, "Swing up control of acrobot using partial feedback linearization," in *Symposium on Robot Control (SYROCO)*, Italy, 1994.

[2] J. Nakanishi, T. Fukuda, and D. E. Koditschek, "A hybrid swing up controller for a two-link brachiating robot," in *IEEE/ASME International Conference on Advanced Intelligent Mechatronics (AIM)*, Atlanta, USA, 1999.

[3] E. Davies, A. Garlow, S. Farzan, J. Rogers, and A.-P. Hu, "Tarzan: Design, prototyping, and testing of a wire-borne brachiating robot," in *2018 IEEE/RSJ International Conference on Intelligent Robots and Systems (IROS)*, Madrid, Spain, 2018.

[4] M. Javadi, D. Harnack, P. Stocco, S. Kumar, S. Vyas, D. Pizzutilo, and F. Kirchner, "Acromonk: A minimalist underactuated brachiating robot," *IEEE Robotics and Automation Letters(RA-L)*, 2023.

[5] D. Reda, H. Y. Ling, and M. van de Panne, "Learning to brachiate via simplified model imitation," in *SIGGRAPH '22 Conference Proceedings*, Vancouver, BC, Canada, 2022.

[6] J. Ho and S. Ermon, "Generative adversarial imitation learning," in *Advances in neural information processing systems*, vol. 29, 2016, pp. 4565–4573.

[7] T. Fukuda, F. Saito, and F. Arai, "A study on the brachiation type of mobile robot," in *IEEE/RSJ International Conference on Intelligent Robots and Systems (IROS)*, Japan, 1991.

[8] M. W. Spong, "Swing up control of the acrobot," *IEEE Control Systems*, 1994.

[9] J. Nakanishi., T. Fukuda, and D. E. Koditschek, "Preliminary studies of a second generation brachiation robot controller," *Proceedings of the 1997 IEEE Innternational Conference on Robotics and Automation(ICRA)*, 1997.

[10] J. Nakanishi T. Fukuda, and D. E. Koditschek, "Experimental implementation of a "target dynamics" controller on a two-link brachiating robot," in *Proceedings of the 1998 IEEE International Conference on Robotics and Automation (ICRA)*, Leuven, Belgium, 1998.

[11] M. W. Gomes and A. L. Ruina, "A five-link 2d brachiating ape model with life-like zero-energy-cost motions," *Journal of Theoretical Biology*, 2005.

[12] T. Fukuda, S. Kojima, K. Sekiyama, and Y. Hasegawa, "Design method of brachitation controller based on virtual holonomic constraint," in *2007 IEEE/RSJ International Conference on Intelligent Robots and Systems (IROS)*, 2007.

[13] J. Nakanishi and S. Vijayakumar, "Exploiting passive dynamics with variable stiffness actuation in robot brachiation," in *Robotics: Science and Systems (RSS)*, 2013.

[14] S. Yang, Z. Gu, R. Ge, A. M. Johnson, M. Travers, and H. Choset, "Design and implementation of a three-link brachiation robot with optimal control based trajectory tracking controller," *arXiv preprint arXiv:1911.05168*, 2019.

[15] S. Farzan, V. Azimi, A.-P. Hu, and J. Rogers, "Cable estimation-based control for wire-borne underactuated brachiating robots: A combined direct-indirect adaptive robust approach," in *2020 59th IEEE Conference on Decision and Control (CDC)*, Jeju Island, Korea, 2020.

[16] R. Fukaya, T. Kawakami, F. Yamasaki, and K. Tsujita, "Single-rod brachiation robot: Continuous and aerial brachiation with simple structure," in *2022 IEEE/RSJ International Conference on Intelligent Robots and Systems (IROS)*. IEEE, 2022, pp. 11 296–11 302.

[17] DeepMind, "Mujoco menagerie: Collection of robotic models," https://github.com/google-deepmind/mujoco_menagerie, 2023, accessed: July 4, 2025.

[18] J. Nakanishi T. Fukuda, and D. E. Koditschek, "A brachiating robot controller," University of Michigan, Tech. Rep. CSE-TR-40599, 1999.

[19] Z. Cheng, H. Cheng, and H. Xu, "Deep reinforcement learning based brachiation control for two-link bio-primate robot," in *2018 IEEE International Conference on Robotics and Biomimetics (ROBIO)*, Kuala Lumpur, Malaysia, 2018.